

# Different Molecules Experience Different Polarities at the Air/Water Interface\*\*

Sobhan Sen, Shoichi Yamaguchi, and Tahei Tahara\*

An interface is the boundary that separates two bulk phases. The interfacial regions have the length scale of only a few nanometers, but are essential environments for many fundamental physicochemical and biological processes to take place.<sup>[1–4]</sup> The distinct anisotropy across the interface greatly influences the properties of interfacial molecules, such as structure, density, viscosity, polarity, and dynamics, and makes the interfacial region markedly different from the constituent bulk phases.<sup>[3–16]</sup> Solute molecules adsorbed at liquid interfaces experience significantly different local environments from those in the constituent bulk media, which makes chemistry at the interface markedly different.<sup>[3–7,9–15]</sup> In spite of the importance of chemistry at interfaces, however, our knowledge about the molecular behavior at interfaces is very limited compared with that for molecules in the bulk phase.

Polarity at the liquid interface is a concept that expresses the ability of interfacial solvent molecules to stabilize polar solute molecules at the interface,<sup>[9,10,15]</sup> which is analogous to the fundamental concept of the polarity of bulk solvents.<sup>[17]</sup> Several pioneering attempts have been made to evaluate the polarity of liquid interfaces, and a generalized interfacial polarity scale has been proposed which claims that the polarity of a liquid interface is the arithmetic average of the polarity of two constituent bulk phases.<sup>[9,10]</sup> This argument was made based on the electronic spectra of solvatochromic molecules at the interface measured with scanning-type resonant second harmonic generation (SHG) spectroscopy.<sup>[9–15]</sup> Nevertheless, the limited quality of electronic spectra obtainable with SHG spectroscopy has hindered further quantitative study of solute–solvent interactions at liquid interfaces.

Recently, we have developed multiplex electronic sum frequency generation (ESFG) spectroscopy (Figure 1), in which a narrowband near-IR laser pulse ( $\omega_1$ ) and a broadband white-light continuum ( $\omega_2$ ) are irradiated on interfaces and the entire ESFG ( $\omega_1 + \omega_2$ ) spectrum is detected with a multichannel detector in a single measurement<sup>[18–21]</sup> (see the Supporting Information for experimental details). This new

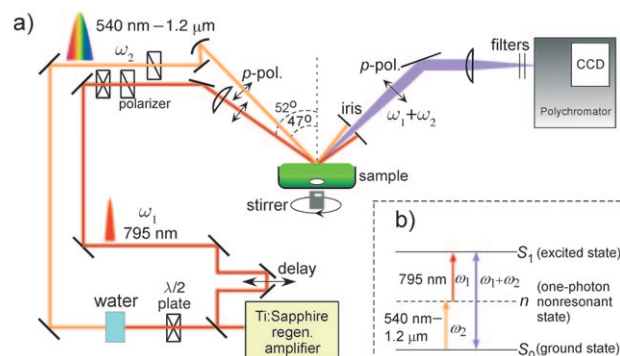


**Figure 1.** a) Ray diagram of multiplex ESFG spectroscopy. All the ESFG spectra were recorded with the *p*-polarization of  $\omega_1$ ,  $\omega_2$ , and  $\omega_1 + \omega_2$ .  $\omega_1$  is 795 nm (bandwidth: 160  $\text{cm}^{-1}$ ) and  $\omega_2$  is a white-light continuum (540 nm–1.2  $\mu\text{m}$ ). b) Energy diagram of the two-photon single-resonant ESFG process. The  $S_1$  state is nonresonant over the entire one-photon wavelength regions of  $\omega_1$  (795 nm) and  $\omega_2$  (540 nm–1.2  $\mu\text{m}$ ). See the Supporting Information for experimental details.

second-order nonlinear spectroscopy technique provides precise and quantitative interfacial electronic spectra with an unprecedented high signal-to-noise ratio that is comparable to the absorption spectra of molecules in the bulk solutions. ESFG spectroscopy enables us to intensively study the properties of molecules at liquid interfaces by electronic spectroscopy at the same level as for molecules in the bulk solutions.<sup>[18–21]</sup>

Herein, we report a systematic study on solvatochromism at the air/water interface by using ESFG spectroscopy. This work clearly shows that the electronic spectra of a series of molecules exhibit significantly different solvatochromic shifts at the *same* air/water interface, thus demonstrating that different molecules experience different effective polarity at the air/water interface.

Coumarin dyes are a group of molecules that have the structure of coumarin (2-chromenone) as their common framework and are well known as prototypical solvatochromic molecules. They have been extensively used in various photophysical/chemical studies as standard probes to monitor the polarity of environments.<sup>[11,12,22,23]</sup> Figure 2a shows the electronic spectra of five coumarin derivatives (C-314, C-338, C-6H, C-1, C-110) at the air/water interface measured by ESFG spectroscopy (experimental details for the acquisition of ESFG spectra are described in the Supporting Information). The absorption spectra of the coumarins in various bulk solvents are also shown in Figure 2a for comparison. Because the ESFG spectra are measured under two-photon resonant and one-photon nonresonant conditions, the observed spectra

[\*] Dr. S. Sen, Dr. S. Yamaguchi, Dr. T. Tahara  
Molecular Spectroscopy Laboratory, Advanced Science Institute (ASI), RIKEN, 2-1 Hirosawa, Wako 351-0198 (Japan)  
Fax: (+81) 48-467-4539  
<http://www.riken.jp/lab-www/spectroscopy/en/index.html>  
E-mail: tahei@riken.jp

[\*\*] This work was supported by a Grant-in-Aid for Scientific Research (A) (No. 19205005) from JSPS and a Grant-in-Aid for Science Research on Priority Area (No. 19056009) from MEXT. S.S. thanks JSPS for a postdoctoral fellowship.

Supporting Information for this article is available on the WWW under <http://dx.doi.org/10.1002/anie.200901094>.

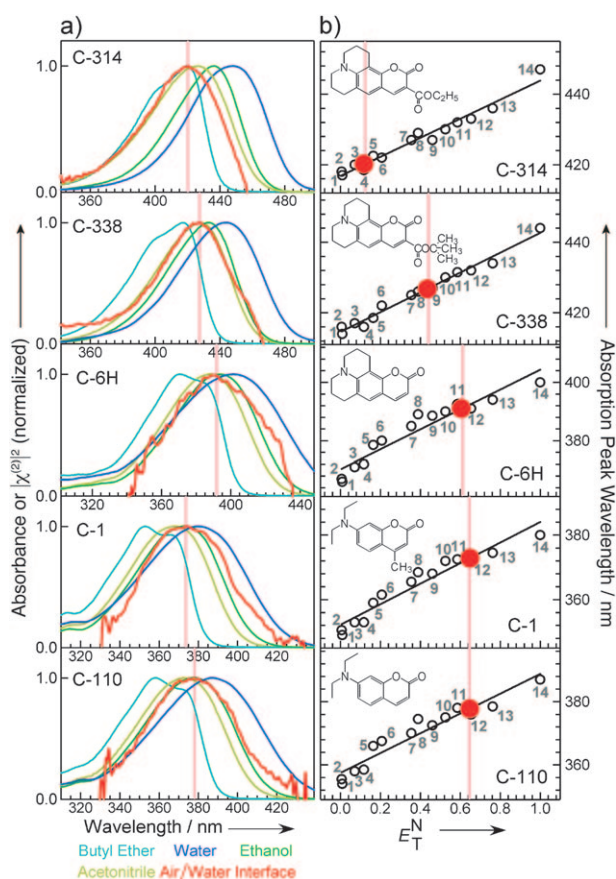


**Figure 2.** a) Two-photon single-resonant ESFG spectra of the coumarins at the air/water interface (red curves) and the absorption spectra of the coumarins in bulk solvents (light blue: butyl ether, greenish yellow: acetonitrile, green: ethanol, blue: water). Vertical pink lines indicate the peak positions of the ESFG spectra. b) Plots of the peak wavelengths of the  $S_1 \leftarrow S_0$  transitions of the coumarins in 14 solvents against the solvent  $E_T^N$  values (open circles). The solvents plotted are hexane (1), cyclohexane (2), butyl ether (3), ethyl ether (4), 1,4-dioxane (5), THF (6), acetone (7), 2-methyl 2-propanol (8), acetonitrile (9), 1-decanol (10), 1-butanol (11), ethanol (12), methanol (13), and water (14). Solid black lines show the best linear fits to these data. The peak wavelengths of the ESFG spectra at the air/water interface are plotted on the lines of the best linear fits (solid red circles). Vertical pink lines show the corresponding  $E_T^N$  values indicated by each coumarin at the air/water interface. Molecular structures of the coumarins are shown in the upper left corner of each panel. See the Supporting Information for experimental details.

directly represent the  $S_1 \leftarrow S_0$  electronic spectra of the molecules at the interface when they are plotted against the  $\omega_1 + \omega_2$  wavelength. In Figure 2a, the  $S_1 \leftarrow S_0$  electronic spectra for all the coumarins at the air/water interface exhibit transitions that lie in between their transition energies in nonpolar hexane and polar water. This fits our intuition that some parts of the interfacial molecules are exposed to the nonpolar air and some parts are surrounded by the polar water, and hence the molecules experience intermediate environments between the two bulk media. Upon taking a closer look, however, we readily notice that the structurally different coumarin molecules exhibit different solvatochromic shifts at the air/water interface. For example, at the

interface, C-314 shows a spectral peak ( $\lambda_{\max}$ ) at around 420 nm that corresponds to its transition energy in bulk butyl ether, whereas the solvatochromic shift of C-338 ( $\lambda_{\max} \approx 428$  nm) indicates a polar environment at the interface similar to bulk acetonitrile. C-6H exhibits  $\lambda_{\max}$  of approximately 392 nm, which is comparable to its transition energy in 1-butanol, and C-1 ( $\lambda_{\max} \approx 373$  nm) and C-110 ( $\lambda_{\max} \approx 378$  nm) exhibit peaks at almost the same position as in bulk ethanol.

The generalized interfacial polarity scale claims that the effective polarity at an interface is the arithmetic average of the polarity of the two constituent bulk phases,<sup>[9,10]</sup> and that the effective polarity of the air/water interface is almost equivalent to the polarity of bulk butyl ether.<sup>[9–11]</sup> Although the ESFG spectrum of C-314 exhibits the peak at an energy equivalent to that in bulk butyl ether,<sup>[11,12]</sup> the present ESFG measurements revealed that this agreement for C-314 is more or less accidental. The effective interfacial polarities indicated by the solvatochromic shifts of the probe molecules are noticeably different from each other in spite of the similarity in the basic molecular structures.

To quantitatively discuss the solvatochromic shifts observed at the air/water interface, we analyzed the data using the  $E_T^N$  polarity scale, which is the normalized version of the  $E_T(30)$  scale with water polarity defined as unity.<sup>[17]</sup> Note that we use this  $E_T^N$  polarity scale as a scale for the total stabilization energy gained by each solute molecule from the surrounding environment at the air/water interface, although  $E_T^N$  was originally defined to represent the polarity inherent to bulk solvents. We plotted the peak wavelengths of the linear absorption spectra (recorded in 14 different bulk solvents) against the solvent  $E_T^N$  values in Figure 2b, and obtained the best linear fits (solid black lines). With the peak positions of the ESFG spectra plotted on the lines of the best linear fits, we obtained  $E_T^N$  values of 0.12, 0.43, 0.61, 0.64, and 0.64 for C-314, C-338, C-6H, C-1, and C-110, respectively, at the air/water interface. This quantifies the different polarity sensed by the different coumarins, and therefore the different stabilization energy gained by the different coumarins at the air/water interface (notably the peak positions of the ESFG spectra can be directly compared with those of linear absorption spectra in the present case; see the Supporting Information for comparison of the linear absorption and ESFG spectra).

Molecular dynamics (MD) simulation studies recently predicted that the position and orientation of solute molecules at the interface are important factors that determine the solvent accessibility to the solute molecules, and hence they can cause significantly different local solvation environments around the solutes at the interface.<sup>[3,5–7]</sup> One intuitive possibility is that, depending on the molecular hydrophobicity, different coumarin molecules may stay at different positions along the interface normal, and acquire stabilization energy different from that of the surrounding environment. In fact, Steel and Walker showed that molecules (other than coumarins) with different hydrophobicities experience different stabilization at the *same* liquid/liquid interface depending on their position along the interface normal.<sup>[13,15]</sup> They synthesized “molecular rulers” that consisted of the anionic sulfate group attached to a hydrophobic solvatochromic

probe through alkyl spacers of different length, and showed that the probes can experience different solvation environments at the same liquid/liquid interface depending on the length of the alkyl spacers.<sup>[13]</sup> For the coumarins in the present study, water solubility indicates the following order of hydrophobicity: C-338 > C-6H > C-314 > C-1  $\geq$  C-110 (from the most to the least hydrophobic; see the Supporting Information.) This order does not fit the order of the  $E_T^N$  value indicated by each molecule at the interface: C-314 (0.12) < C-338 (0.43) < C-6H (0.61)  $\approx$  C-1 (0.64) = C-110 (0.64). In fact, the most hydrophobic (the least water-soluble) coumarin C-338 experiences an intermediate polar environment ( $E_T^N = 0.43$ ), whereas the moderately water-soluble C-314 senses the most nonpolar ( $E_T^N = 0.12$ ) environment at the air/water interface. This result suggests that the overall hydrophobicity, and hence difference in the vertical position, is not the predominant factor in the observed variation of the effective polarity sensed by the coumarins at the interface.

To examine the contribution of the molecular orientation, we performed polarization measurements of resonant SHG at a single wavelength.<sup>[24–27]</sup> Figure 3b shows the input polar-

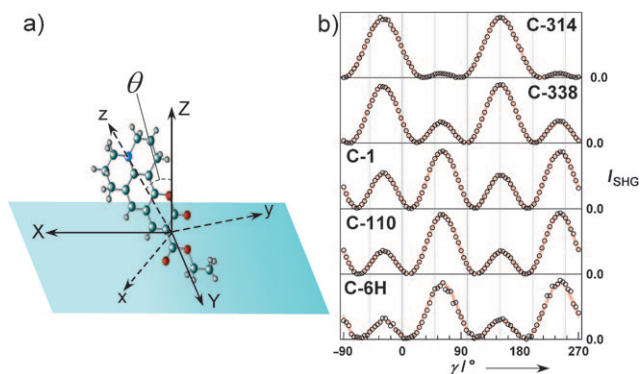


**Figure 3.** a) Molecular orientation at the air/water interface showing the definition of the tilt angle ( $\theta$ ), the laboratory axes ( $X, Y, Z$ ), and the molecular axes ( $x, y, z$ ). The tilt angle  $\theta$  is defined as the angle between the  $S_1 \leftarrow S_0$  transition dipole moment (parallel with the molecular  $z$  axis) and the interface normal (parallel with the laboratory  $Z$  axis). b) The  $\gamma$  dependence of the resonant SHG intensities ( $I_{\text{SHG}}$ ) of the coumarins at the air/water interface (analyzer angle at  $45^\circ$ ,  $\gamma$  represents the input polarization angle). Open black circles are the raw data points and red lines are the best fits. The photon energy of the fundamental input was tuned at the half value of the peak energy of the ESFG spectrum of each coumarin at the interface.  $0^\circ$  corresponds to  $p$ -polarization and  $90^\circ$  to  $s$ -polarization. See the Supporting Information for more details.

ization dependence of the SHG intensity measured at a detection analyzer angle of  $45^\circ$  (see the Supporting Information for experimental details and SHG data for other detection analyzer angles). A glimpse at the raw data reveals that they are very similar for C-1, C-110, and C-6H, which indicates similar  $E_T^N$  values, and the data for C-314 and C-338 are different from one to another as well as from the others. This suggests a correlation between the effective polarity indicated by each coumarin and the molecular orientation at the air/water interface. We carried out quantitative analysis of the polarization-dependent SHG data, and evaluated the tilt

angle ( $\theta$ ) of the  $S_1 \leftarrow S_0$  transition dipole moment (parallel with the molecular  $z$  axis) against the interface normal (parallel with the laboratory  $Z$  axis) assuming a sharp ( $\delta$  function) orientational distribution for each molecule (Figure 3a;<sup>[25–27]</sup> see the Supporting Information for analysis of the SHG data and calculation of orientation angles). The tilt angles obtained for the coumarins followed the sequence: C-314 ( $64^\circ$ ) > C-338 ( $57^\circ$ ) > C-1 ( $52^\circ$ ) > C-110 ( $50^\circ$ ) > C-6H ( $49^\circ$ ). This order shows good correlation with the order of the effective polarity indicated by each molecule at the air/water interface (C-314 < C-338 < C-6H  $\approx$  C-1 = C-110). This result reveals that the molecular orientation is the predominant factor giving rise to the variation of the effective polarity sensed by each probe molecule at the interface.

Although the five molecules selected for this work share the common coumarin framework, they have different molecular structures. It is highly likely that site-specific interaction between the polar substituent and interfacial water acts as an “anchor” for the molecules, thus affecting their orientations. Owing to the difference in this anchoring effect, the coumarins can orient in different ways so that they have different accessibility to water at the interface (Figure 4). The ESFG data indicate that the most tilted, C-

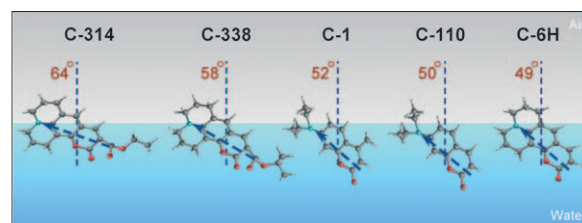


**Figure 4.** Different orientations of the coumarin molecules at the air/water interface. The arrows indicate the  $S_1 \leftarrow S_0$  transition dipole moments of the coumarins.

314 ( $\theta = 64^\circ$ ), senses the most nonpolar environment ( $E_T^N = 0.12$ ) and gains the least stabilization energy at the interface. This is probably because C-314 orients in such a way that not only the upper part of the molecule is exposed to the nonpolar air, but also the lower part of the molecule has limited accessibility to the polar water (see Figure 4). The less tilted C-338 ( $\theta = 57^\circ$ ) subsequently increases the water accessibility to its lower part and hence senses a more polar environment ( $E_T^N = 0.43$ ), which causes a larger solvatochromic shift towards the low-energy side (see also Figure 2). C-1 ( $52^\circ$ ), C-110 ( $50^\circ$ ), and C-6H ( $49^\circ$ ) are least tilted from the interface normal, which further increases the extent of the solute–water interaction and leads to the further red shifts of their electronic transitions ( $E_T^N = 0.61$ – $0.64$ ). We consider that this is a possible mechanism that gives rise to the clear correlation between the molecular orientation and the effective local polarity indicated by each coumarin at the air/water interface. Although the difference in the hydrophobicity may affect the absolute vertical positions of coumarins to some extent, the observed orientation–polarity correlation indicates that the differences in molecular orientations are the predominant factor for the probe molecules to experience different



effective local solvation environments at the air/water interface.

Because ESFG spectroscopy provides high-quality interfacial electronic spectra comparable to the absorption spectra in solution, we can also discuss the bandwidth of the electronic transition at the air/water interface. As Figure 2a shows, the obtained interfacial electronic spectra look very similar to the absorption spectra in polar bulk liquids in terms of their spectral widths and line shapes. The bandwidths of the interfacial electronic spectra are as broad as those of the absorption spectra in highly polar bulk liquids such as methanol or ethanol. The broad bandwidths of the ESFG spectra indicate that the widely distributed solvation sites are also present at the air/water interface, mainly as a result of thermal roughness and solvent fluctuation at the interface. More quantitative discussion on the line shape will be carried out for imaginary  $\chi^{(2)}$  spectra that are obtainable with heterodyne-detected ESFG developed recently in our group.<sup>[28]</sup>

Lastly, we discuss the validity of the assumption of the  $\delta$ -function orientation distribution that we adopted in the analysis of our polarization SHG data. Recent MD simulations predicted that molecules at the air/water interface have a certain orientational distribution.<sup>[5,7,16]</sup> To check the effect of this orientational distribution, we also evaluated the mean tilt angles by assuming different widths of Gaussian distributions of the orientations.<sup>[29]</sup> Table 1 shows the mean tilt angles of the

**Table 1:** Mean tilt angles of the coumarins calculated assuming the Gaussian orientation distributions of different widths. See the Supporting Information for details of the width-dependent orientation calculation.

Distribution width $\sigma$ [°]	Mean tilt angle [°]				
	C-314	C-338	C-1	C-110	C-6H
0 <sup>[a]</sup>	64	57	52	50	49
5	64	57	52	50	49
10	64	57	52	50	49
15	65	58	53	51	50
20	66	58	55	53	52

[a]  $\delta$ -function distribution.

coumarins obtained with the different widths of the Gaussian distributions assumed (see the Supporting Information for details of this calculation). From Table 1, it can be seen that for a particular width value of the Gaussian distribution, the mean tilt angles of the coumarins follow the same trend as that seen for the tilt angles determined experimentally by assuming the  $\delta$ -function distribution. This implies that as long as the distribution widths are similar among the molecules studied, the good correlation between the effective polarities and mean tilt angles of the molecules is persistent, even if there is some orientational distribution of the molecules at the air/water interface.

In conclusion, we have demonstrated that the local solvation environment around the solute molecule at the air/water interface is significantly different, even among

molecules that have similar molecular structures. This finding implies that the polarity of the air/water interface does not have a straightforward meaning because it cannot be determined as a value independent of the solute molecule. The stabilization energy that the solute molecule gains from solvation at the interface changes significantly with even a small change in the conditions, such as the tilt angle of the molecule at the interface. This is one of the manifestations of the rich but complicated features of chemistry at the water interface, which plays a crucial role in wide areas of chemistry, biochemistry, and atmospheric science.

Received: February 26, 2009

Revised: June 16, 2009

**Keywords:** electronic spectroscopy · interfaces · nonlinear optics · polarity · solvatochromism

- [1] B. J. Finlayson-Pitts, J. N. Pitts, Jr. in *Chemistry of the Upper and Lower Atmosphere*, Academic Press, San Diego, **2000**.
- [2] A. G. Volkov in *Interfacial Catalysis*, Marcel Dekker, New York, **2003**.
- [3] I. Benjamin, *Chem. Rev.* **2006**, *106*, 1212.
- [4] K. B. Eisenthal, *Chem. Rev.* **1996**, *96*, 1343.
- [5] D. Michael, I. Benjamin, *J. Phys. Chem. B* **1998**, *102*, 5145.
- [6] I. Benjamin, *J. Phys. Chem. A* **1998**, *102*, 9500.
- [7] A. Pohorille, I. Benjamin, *J. Chem. Phys.* **1991**, *94*, 5599.
- [8] S. Senapati, M. L. Berkowitz, *Phys. Rev. Lett.* **2001**, *87*, 176101.
- [9] H. Wang, E. Borguet, K. B. Eisenthal, *J. Phys. Chem. A* **1997**, *101*, 713.
- [10] H. Wang, E. Borguet, K. B. Eisenthal, *J. Phys. Chem. B* **1998**, *102*, 4927.
- [11] D. Zimdars, K. B. Eisenthal, *J. Phys. Chem. B* **2001**, *105*, 3993.
- [12] A. V. Benderskii, K. B. Eisenthal, *J. Phys. Chem. A* **2002**, *106*, 7482.
- [13] W. H. Steel, R. A. Walker, *Nature* **2003**, *424*, 296.
- [14] W. H. Steel, F. Damkaci, R. Nolan, R. A. Walker, *J. Am. Chem. Soc.* **2002**, *124*, 4824.
- [15] W. H. Steel, R. A. Walker, *J. Am. Chem. Soc.* **2003**, *125*, 1132.
- [16] D. A. Pantano, D. Laria, *J. Phys. Chem. B* **2003**, *107*, 2971.
- [17] C. Reichardt, *Chem. Rev.* **1994**, *94*, 2319.
- [18] S. Yamaguchi, T. Tahara, *J. Phys. Chem. B* **2004**, *108*, 19079.
- [19] S. Yamaguchi, T. Tahara, *J. Chem. Phys.* **2006**, *125*, 194711.
- [20] S. Yamaguchi, T. Tahara, *Angew. Chem.* **2007**, *119*, 7753; *Angew. Chem. Int. Ed.* **2007**, *46*, 7609.
- [21] K. Sekiguchi, S. Yamaguchi, T. Tahara, *J. Chem. Phys.* **2008**, *128*, 114715.
- [22] M. L. Horng, J. A. Gardecki, A. Papazyan, M. Maroncelli, *J. Phys. Chem.* **1995**, *99*, 17311.
- [23] R. S. Moog, W. W. Davis, S. G. Ostrowski, G. L. Wilson, *Chem. Phys. Lett.* **1999**, *299*, 265.
- [24] Y. R. Shen in *The Principles of Nonlinear Optics*, Wiley, New York, **1984**.
- [25] A. A. T. Luca, P. Hébert, P. F. Brevet, H. H. Girault, *J. Chem. Soc. Faraday Trans.* **1995**, *91*, 1763.
- [26] W. K. Zhang, H. F. Wang, D. S. Zheng, *Phys. Chem. Chem. Phys.* **2006**, *8*, 4041.
- [27] D. J. Campbell, D. A. Higgins, R. M. Corn, *J. Phys. Chem.* **1990**, *94*, 3681.
- [28] S. Yamaguchi, T. Tahara, *J. Chem. Phys.* **2008**, *129*, 101102.
- [29] G. J. Simpson, K. L. Rowlen, *J. Am. Chem. Soc.* **1999**, *121*, 2635.